Double multiphoton ionization of a model atom

M. S. Pindzola, F. Robicheaux, and P. Gavras
Department of Physics, Auburn University, Auburn, Alabama 36849
(Received 29 August 1996)

A direct solution of the time-dependent Schrödinger equation (TDSE) for a two-electron model atom in a strong electromagnetic field is used to extract probabilities for both single and double electron ionization. For three-photon ionization at a moderately strong intensity, the TDSE calculations find single ionization at 62%, single ionization with excitation at 10%, and double ionization at 3%. The sequential process of escape from an already once ionized atom is found to make a substantial contribution to the double-ionization probability. Multiphoton-ionization probabilities are also obtained from a solution of the time-dependent unrestricted Hartree-Fock (TDUHF) equations for the same model atom. Although in qualitative agreement with the TDSE results, the TDUHF results show significantly less single ionization with excitation and have a different angular distribution for double ionization. [S1050-2947(97)07102-3]

PACS number(s): 32.80.Rm

I. INTRODUCTION

With the development of high-frequency synchrotron light sources, the process of double photoionization in atoms has received considerable attention [1]. The double-photoionization process is defined as the ejection of two electrons following absorption of a single photon. Various theoretical methods have been successful in predicting the strength of the double-photoionization process in atoms and delineating the mechanisms: (i) direct double ionization, (ii) inner-shell ionization followed by Auger emission, and (iii) photoexcitation followed by double Auger emission. For direct double ionization of helium [1], the peak of the double-photoionization cross section occurs at 100-eV photon energy and is approximately 12 kb, about 2.5% of the single-photoionization cross section at that energy. The agreement between theory [2–7] and experiment is reasonably good.

With the development of high-intensity lasers, the process of double multiphoton ionization in atoms has also attracted attention [8]. The double-multiphoton-ionization process may be defined as the ejection of two electrons following absorption of multiple photons. For direct double multiphoton ionization of helium [8], the double-ionization rate for 1.59-eV photons at an intensity of 10^{15} W/cm^2 is about 0.2% of the single-ionization rate at the same intensity. Various correlation [9,10] and rescattering [11] mechanisms have been put forward to explain the low-frequency, long-pulse, laser-atom experiments.

In this paper we examine high-frequency, short-pulse, laser-atom interactions leading to single and double ionization by a direct solution of the time-dependent Schrödinger equation (TDSE) for a two-electron model atom. The two-electron model atom has been previously employed to study the multiphoton ionization of He [12,13], the multiphoton detachment of H^- [14,15], the autoionization of He* [16,17], and the multiphoton ionization of H_2 [18,19]. Here the model atom serves several useful purposes. First a TDSE solution of the model atom reflects many of the qualitative features found in full three-dimensional (3D) calculations for the multiphoton ionization of the helium atom [20], at significantly reduced computational expense. Besides providing physical insight into the double-ionization process, the model atom results can be used to examine convergence rates for lattice sizes, mesh intervals, and time steps. Second, various approximate methods can be easily formulated for the model atom. Their range of validity can then be tested by comparison to the direct solution's values for various dynamical observables. In this paper we examine how well time-dependent unrestricted Hartree-Fock (TDUHF) theory handles the double-ionization process. Third, the model atom can provide some guidance for experiment, although caution must be exercised. Because of Hilbert space restrictions, the single-ionization rates for the model atom are an order of magnitude larger than those found in full 3D calculations for the helium atom [12]. However, the dependence of single and double ionization rates on the frequency and intensity of the electromagnetic field may be similar for model and real atoms. The time-dependent theory for the two-electron model atom is reviewed in Sec. II, single- and double-multiphoton-ionization results are presented in Sec. III, and a brief summary is found in Sec. IV.

II. THEORY

A. The model atom

The Hamiltonian for a two-electron model atom [12,14] is given by (in atomic units)

$$H_0 = -\frac{1}{2}\frac{d^2}{dx^2} - \frac{1}{2}\frac{d^2}{dy^2} - \frac{Z}{\sqrt{c+x^2}} - \frac{Z}{\sqrt{c+y^2}} + \frac{1}{\sqrt{c+(x-y)^2}}, \tag{1}$$

where x and y are the coordinate positions of each electron, a nucleus of charge $Z=2$ is located at $x=y=0$, and c is an arbitrary constant used to soften the singularity of the potential. The potential energy of the atomic Hamiltonian, H_0, is shown in Fig. 1. The potential ridge is along a line in the xy plane at which $x=y$; i.e., where the electron-electron repulsion term is largest.

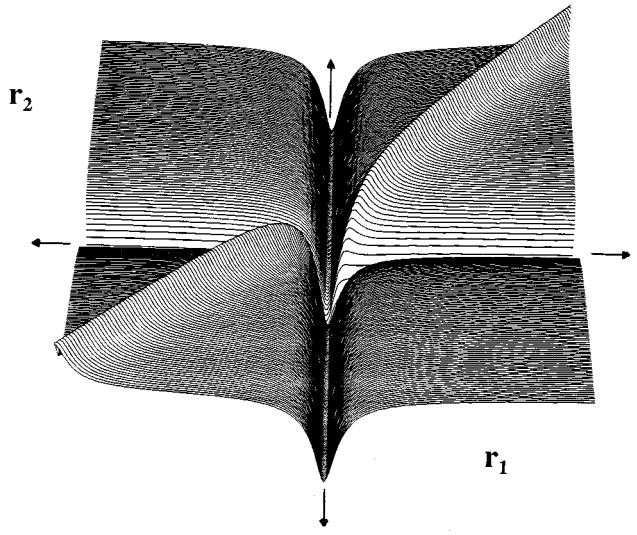

FIG. 1. Atomic potential for the two-electron model atom.

B. Direct solution of the time-dependent Schrödinger equation

To study multiphoton absorption processes, we solve the time-dependent Schrödinger equation

$$i\,\frac{\partial\psi(x,y,t)}{\partial t}=[H_0+V(t)]\psi(x,y,t), \tag{2}$$

where

$$V(t)=E(t)(x+y)\sin(\omega t), \tag{3}$$

$E(t)$ is the field amplitude, and ω is the field frequency. Other choices for the gauge of the electromagnetic field are available [21]. Lattice techniques are used to obtain a discrete representation of the wave function and all operators on a two-dimensional grid. For finite differences, local operators become diagonal matrices and derivative operators, such as the kinetic energy, have lattice representations in terms of banded matrices. The time evolution of the wave function may be approximated by an implicit Peaceman-Rachford propagator [22].

C. Solution of the time-dependent unrestricted Hartree-Fock equations

We first assume that the time evolution of the ground state of the model atom may be described by a symmetrized product wave function:

$$\psi(x,y,t)=\sqrt{\tfrac{1}{2}}[u(x,t)v(y,t)+v(x,t)u(y,t)], \tag{4}$$

where total antisymmetrization of the wave function is obtained by multiplying the symmetric space function by an antisymmetric spin function. Then the variationally derived [13] time-dependent unrestricted Hartree-Fock equations for the nonorthogonal single-particle orbitals, $u(x,t)$ and $v(x,t)$, are given by

$$i\,\frac{\partial u}{\partial t}=h_{11}u+h_{12}v, \tag{5}$$

$$i\,\frac{\partial v}{\partial t}=h_{21}u+h_{22}v, \tag{6}$$

where

$$h_{11}=f+N+\frac{\langle v|f|v\rangle+\langle v|g|v\rangle-\lambda^*\langle u|f|v\rangle-\lambda^*\langle u|g|v\rangle+i\lambda^*\langle u|\partial v/\partial t\rangle}{1-\lambda^*\lambda}, \tag{7}$$

$$h_{12}=\frac{\langle v|f|u\rangle+\langle v|g|u\rangle-\lambda^*\langle u|f|u\rangle-\lambda^*\langle u|g|u\rangle-i\langle v|\partial u/\partial t\rangle}{1-\lambda^*\lambda}, \tag{8}$$

$$h_{21}=\frac{\langle u|f|v\rangle+\langle u|g|v\rangle-\lambda\langle u|f|v\rangle-\lambda\langle v|g|v\rangle-i\langle u|\partial v/\partial t\rangle}{1-\lambda^*\lambda}, \tag{9}$$

$$h_{22}=f+N+\frac{\langle u|f|u\rangle+\langle u|g|u\rangle-\lambda\langle v|f|u\rangle-\lambda\langle v|g|u\rangle+i\lambda\langle v|\partial u/\partial t\rangle}{1-\lambda^*\lambda}. \tag{10}$$

The one- and two-particle operators are given by

$$f=-\frac{1}{2}\frac{d^2}{dx^2}-\frac{Z}{\sqrt{c+x^2}}+E(t)x\,\sin(\omega t) \tag{11}$$

and

$$g=\frac{1}{\sqrt{c+(x-y)^2}}, \tag{12}$$

while the matrix elements of the f operator are c numbers, the matrix elements of the g operator are direct and exchange potential terms, and the overlap integral $\lambda=\langle u|v\rangle$. The normalization term is given by

$$N=\frac{i\lambda\langle v|\partial u/\partial t\rangle+i\lambda^*\langle u|\partial v/\partial t\rangle}{1+\lambda^*\lambda}-E, \tag{13}$$

and the total energy is given by

$$E=\frac{\langle u|f|u\rangle+\langle v|f|v\rangle+\lambda^*\langle u|f|v\rangle+\lambda\langle v|f|u\rangle+\langle uv|g|uv\rangle+\langle uv|g|vu\rangle}{1+\lambda^*\lambda}. \tag{14}$$

Lattice techniques are used to solve the time-dependent unrestricted Hartree-Fock equations on a one-dimensional grid. The reduced dimensionality of the numerical problem is somewhat mitigated by the sheer number of operators and c numbers that need to be updated per time step. The time evolution of the wave function may be approximated by an explicit Taylor series propagator [23].

D. Single- and double-ionization probabilities

The total wave function at time $t=T$ following the laser pulse is used to calculate various multiphoton absorption probabilities [15]. The ground-state probability is given by

$$P_{\rm gnd}=|\langle\psi(x,y,t=0)|\psi(x,y,t=T)\rangle|^2. \tag{15}$$

A complete set of field-free bound and continuum states for the atomic ion may be obtained by diagonalization of the one-electron Hamiltonian on the grid. The probability of finding one electron in the bound state ϕ_m and the other electron in the bound state ϕ_n is given by

$$P_{mn}=\left|\int dx\int dy\,\phi_m(x)\phi_n(y)\psi(x,y,t=T)\right|^2. \tag{16}$$

The probability of finding one electron in the bound state ϕ_n and the other electron in the continuum is given by

$$P_{nk}=2\left(\int dx\left|\int dy\,\phi_n(y)\psi(x,y,t=T)\right|^2-\sum_m P_{mn}\right). \tag{17}$$

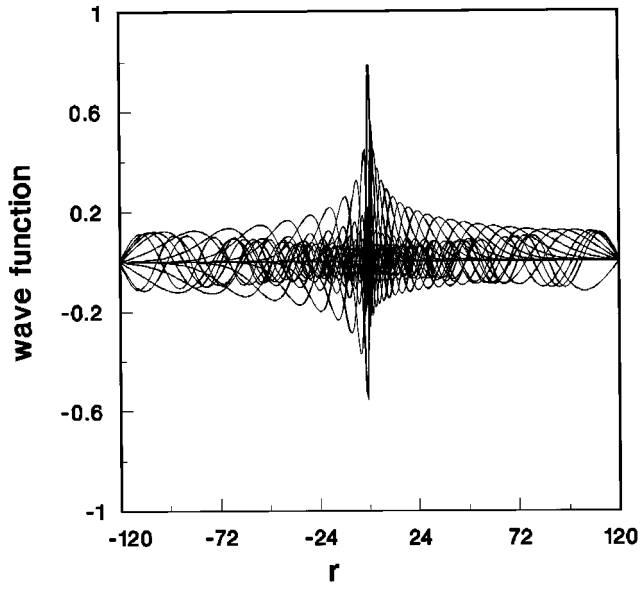

FIG. 2. Field-free bound eigenstates for a lattice range of ±120 and a spacing of 0.4. Distance is in atomic units (1 a.u.$=5.29\times10^{-9}$ cm).

Thus the probability of single ionization is P_{1k} and the probability of ionization with excitation to the first excited state is P_{2k}. The double-ionization probability is given by

$$P_{kk}=1-\sum_n P_{nk}-\sum_m\sum_n P_{mn}. \tag{18}$$

III. MULTIPHOTON-IONIZATION RESULTS

In previous work [13] we investigated the single multiphoton ionization of the model atom at an intensity of 1.0×10^{15} W/cm^2 and a photon energy of 10.0 eV, corresponding to three-photon ionization. The TDSE and TDUHF methods were found to be in good agreement for the depletion of the ground state, as calculated from Eq. (15). To calculate the single-ionization, single ionization with excitation, and double-ionization probabilities from Eqs. (17) and (18), the time dependence of the laser pulse was assumed to be given by

$$E(t)=E_0\sin^2(\pi t/T), \tag{19}$$

with $T=10$ laser cycles. With a uniform grid spacing of 0.4, we choose lattice ranges of ±30, ±60, and ±120 to test the convergence of the bound and continuum probabilities. The field-free bound eigenstates, $\phi_n(x)$, obtained by diagonalization, numbers 12, 18, and 26 for the lattice ranges ±30, ±60, and ±120. For the ±120 lattice, the bound eigenstates are shown in Fig. 2, while their corresponding eigenenergies are given in Table I. There are an additional 139, 283, and 575 field-free continuum eigenstates associated with the three choices for lattice size. As shown in Table II the convergence of the probabilities is quite rapid with respect to lattice range. For the smallest lattice range of ±30, an examination of the probability density contour plots reveals a large amount of reflection from the lattice boundary. However,

TABLE I. Field-free bound eigenenergies for a lattice range of ±120 and a spacing of 0.4.

Number	Energy (eV)	Number	Energy (eV)
1	−52.4740	14	−0.9994
2	−25.0586	15	−0.8780
3	−14.5642	16	−0.7755
4	−9.2847	17	−0.6915
5	−6.4579	18	−0.6190
6	−4.7049	19	−0.5577
7	−3.5971	20	−0.5007
8	−2.8224	21	−0.4448
9	−2.2830	22	−0.3828
10	−1.8764	23	−0.3153
11	−1.5751	24	−0.2389
12	−1.3363	25	−0.1572
13	−1.1514	26	−0.0671

TABLE II. Multiphoton ionization of a model atom at an intensity of 1.0×10^{15} W/cm^2.

	TDSE (ω=10 eV) range ±30	TDSE (ω=10 eV) range ±60	TDSE (ω=10 eV) range ±120
$P_{\rm gnd}$	0.724	0.725	0.725
P_{11}	0.695	0.699	0.699
$\sum_n (P_{1n}+P_{n1})$	0.805	0.770	0.766
$\sum_m \sum_n P_{mn}$	0.825	0.779	0.776
P_{1k}	0.161	0.212	0.215
P_{2k}	0.004	0.002	0.002
P_{3k}	0.003	0.002	0.002
$\sum_n P_{nk}$	0.174	0.221	0.224
P_{kk}	0.001	0.000	0.000

TABLE III. Multiphoton ionization of a model atom at an intensity of 1.0×10^{15} W/cm^2.

	TDSE (ω=10 eV) range ±120	TDUHF (ω=10 eV) range ±120
$P_{\rm gnd}$	0.725	0.687
P_{11}	0.699	0.677
$\sum_n (P_{1n}+P_{n1})$	0.766	0.814
$\sum_m \sum_n P_{mn}$	0.776	0.817
P_{1k}	0.215	0.178
P_{2k}	0.002	0.000
P_{3k}	0.002	0.002
$\sum_n P_{nk}$	0.224	0.182
P_{kk}	0.000	0.001

this reflection does not appear to have a major effect on the probabilities of interest for single- and double-multiphoton ionization.

We now turn to the comparison of the TDSE and TDUHF methods for the various bound and continuum probabilities. With a choice of $c=0.55$ the total energy of the ground state on the two-dimensional lattice is -2.908, while the unrestricted Hartree-Fock approximation yields -2.905. The experimental removal energy for both electrons in the real helium atom is -2.902. Following the projections at $t=T$, the probabilities are presented in Table III for the largest lattice range of ±120. Since P_{11} uses an approximation to the ground state obtained by forming the product of two $1s$ ion orbitals, it differs somewhat from $P_{\rm gnd}$ for both methods. By taking the difference between P_{11} and $\Sigma_n(P_{1n}+P_{n1})$ we find that the TDUHF method predicts about twice as much excitation to the excited states leading to the $1s$ ionization limit as the TDSE method: 14% versus 7%. Of course, the differences that exist between the unrestricted Hartree-Fock excited-state spectrum and the exact solution of Schrödinger's equation within the model atom are accentuated by the Stark-induced shifts into two or three photon resonance. Both methods are in fair agreement as to the magnitude of single ionization from the ground state (around 20%) and both methods agree that there is very little double multiphoton ionization at the originally chosen intensity and photon energy for a 10 cycle laser pulse.

It is interesting to see what happens to the model atom when the intensity is doubled to 2.0×10^{15} W/cm^2. The bound and continuum probabilities are given in Table IV for the TDSE and TDUHF methods. At a photon energy of 10 eV both methods show only a small increase in the single ionization from the ground state (around 25%). Although the ground state shows a substantial depletion at this higher intensity, excitation to the excited states leading to the $1s$ ionization limit now dominates the probability flows at approximately 45%. The Stark-induced shifts of the atomic levels have changed the nonresonant three-photon ionization process into a resonant four-photon ionization process. Three-

TABLE IV. Multiphoton ionization of a model atom at an intensity of 2.0×10^{15} W/cm^2.

	TDSE (ω=10 eV) range ±120	TDUHF (ω=10 eV) range ±120	TDSE (ω=11 eV) range ±120	TDUHF (ω=11 eV) range ±120
$P_{\rm gnd}$	0.225	0.217	0.229	0.293
P_{11}	0.215	0.214	0.264	0.269
$\sum_n (P_{1n}+P_{n1})$	0.660	0.715	0.421	0.371
$\sum_n \sum_m P_{nm}$	0.671	0.735	0.430	0.374
P_{1k}	0.275	0.216	0.507	0.597
P_{2k}	0.009	0.004	0.009	0.004
P_{3k}	0.015	0.001	0.010	0.013
$\sum_n P_{nk}$	0.322	0.253	0.557	0.617
P_{kk}	0.007	0.013	0.014	0.009

TABLE V. Multiphoton ionization of a model atom at an intensity of 3.0×10^{15} W/cm^2.

	TDSE (ω=11 eV) range $\pm$120	TDSE (ω=11 eV) range $\pm$240	TDUHF (ω=11 eV) range $\pm$120	TDUHF (ω=11 eV) range $\pm$240
P_{gnd}	0.097	0.097	0.128	0.128
P_{11}	0.094	0.094	0.129	0.129
$\sum_n (P_{1n}+P_{n1})$	0.232	0.234	0.190	0.191
$\sum_m \sum_n P_{mn}$	0.240	0.242	0.192	0.194
P_{1k}	0.622	0.620	0.759	0.757
P_{2k}	0.016	0.016	0.003	0.003
P_{3k}	0.015	0.015	0.008	0.008
$\sum_n P_{nk}$	0.724	0.723	0.784	0.783
P_{kk}	0.036	0.035	0.024	0.024

photon absorption is now resonant with the high Rydberg $1snS$ states. To confirm this plateau feature in the ionization rate versus intensity curve at 10 eV, we increased the photon energy to 11 eV. At the increased frequency both methods show a much larger probability associated with single ionization from the ground state (around 55%). Excitation to the $1snS$ excited states has dropped substantially (now around 10%–15%). A more careful examination of the TDSE results reveals a near-two-photon resonance with the $1s2s$ excited state. The zero-field $1s2s$ state, calculated by relaxation with projection on the lattice, is found at 22.3 eV above the ground state. During the 10-cycle laser pulse the model atom executes 1.5 Rabi oscillations between the $1s^2$ ground and $1s2s$ excited states. The peak probability of the $1s2s$ state is found to be around 12%. Finally, both methods agree that the double multiphoton ionization at the doubled intensity is now at the 1% level.

The bound and continuum probabilities for the TDSE and TDUHF methods at an intensity of 3.0×10^{15} W/cm^2 and a photon energy of 11 eV are given in Table V. The TDSE method gives a 62% probability of single ionization from the ground state, while the TDUHF method gives a 76% probability for the same process. The TDSE method finds more ionization with excitation than the TDUHF method; 10% versus 2%. Both methods agree that the double multiphoton ionization at this strongest intensity is now at the 3% level. To check our numerical results we repeated the calculations with a lattice range of $\pm$240, while keeping the same spacing of 0.4. There are now 38 field-free bound eigenstates $\phi_n(x)$ on the larger lattice with the lowest eigenenergies identical to those given in Table I. As shown in Table V there is very little change in the bound and continuum probabilities for either method. We also made further calculations with a lattice range of $\pm$120, while at the same time decreasing the grid spacing to 0.2. This again had little effect on the bound and continuum probabilities.

Final time wave function density plots for the TDSE and TDUHF methods are shown in Figs. 3 and 4 for an intensity of 3.0×10^{15} W/cm^2 and a photon energy of 11 eV. Both figures are dominated by probability flows along the $\pm x$ or $\pm y$ axes, representing single multiphoton ionization. The

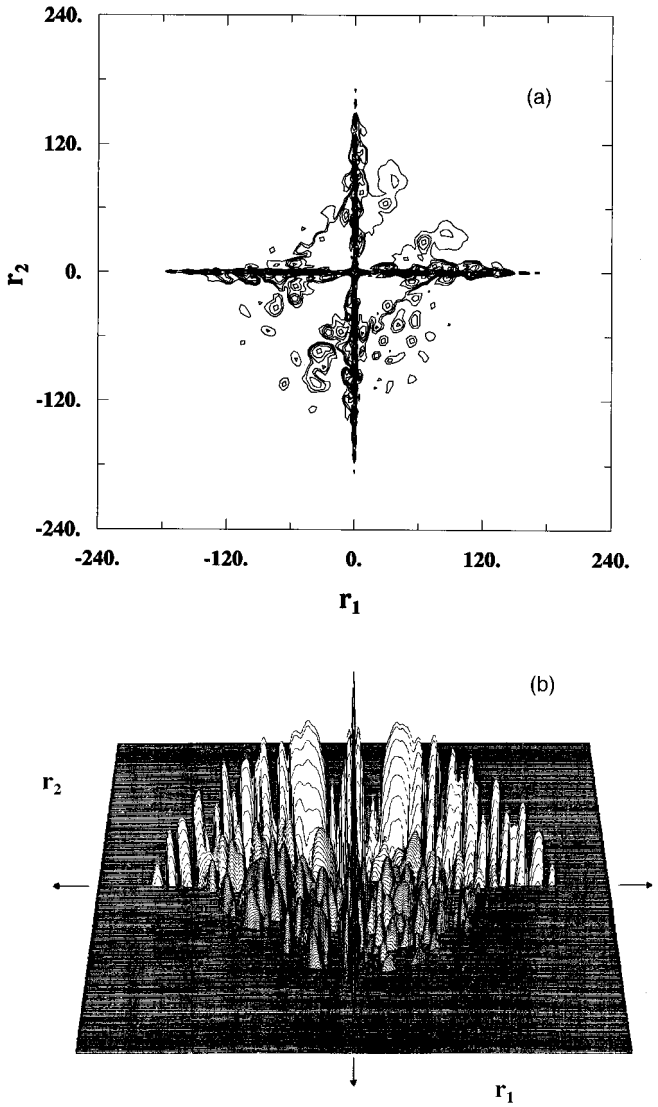

FIG. 3. Contour plot (a) and projection (b) of the final time wave-function density $|\psi(x,y,t=T)|^2$ for the TDSE method at an intensity of 3.0×10^{15} W/cm^2 and photon energy of 11 eV. Distance is in atomic units (1 a.u.$=5.29\times10^{-9}$ cm).

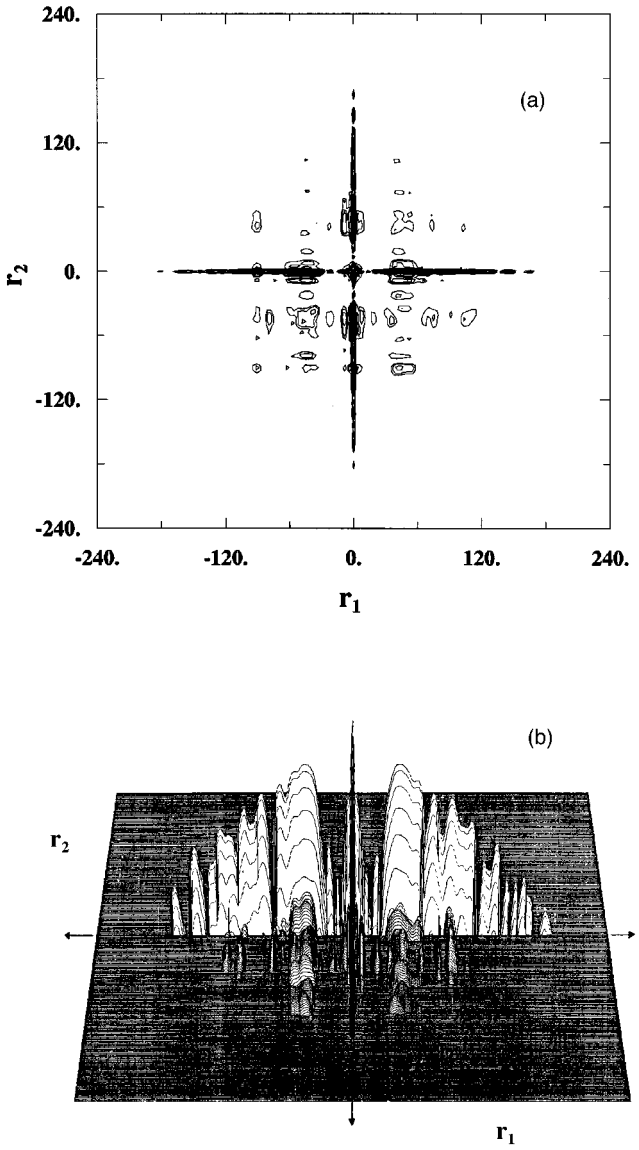

FIG. 4. Contour plot (a) and projection (b) of the final time wave-function density $|\psi(x,y,t=T)|^2$ for the TDUHF method at an intensity of 3.0×10^{15} W/cm^2 and photon energy of 11 eV. Distance is in atomic units (1 a.u.$=5.29\times10^{-9}$ cm).

double ionization is found in the planes between the axes, at much lower strength. The double-ionization peaks in Fig. 3 for the TDSE method avoid the ridge ($x=y$) of the potential. The double-ionization peaks in Fig. 4 for the TDUHF method do not show the ridge avoidance, yielding a density plot that shows more symmetry between the ridge ($x=y$) and flat ($x=-y$) sectors. Thus, even though both methods find roughly the same total probability for double multiphoton ionization, the angular distributions in the xy plane are quite distinct.

To better categorize the type of double multiphoton ionization present, we carried out a one-dimensional TDSE calculation for the multiphoton ionization of the model atomic ion at an intensity of 3.0×10^{15} W/cm^2 and a photon energy of 11 eV. We used the same 10-cycle laser pulse and identical lattice ranges. At least five photons are needed to ionize the model atomic ion (ionization potential of 52.4740 eV).

TABLE VI. Multiphoton ionization of a model atomic ion at an intensity of 3.0×10^{15} W/cm^2.

	TDSE ($\omega=11$ eV) range ±120	TDSE ($\omega=11$ eV) range ±240
P_1	0.933	0.933
$\sum_n P_n$	0.964	0.964
P_k	0.036	0.036

The probability of finding the one electron in the bound state ϕ_n is given by

$$P_n=\left|\int dx\ \phi_n(x)\psi(x,t=T)\right|^2, \tag{20}$$

while the probability of finding the one electron in the continuum is given by

$$P_k=1-\sum_n P_n. \tag{21}$$

The bound and continuum probabilities for multiphoton ionization of the ion are given in Table VI. The probability for ionization is at the 3% level. Thus, the double multiphoton ionization of the model atom has a substantial contribution from the sequential process of ionization of the atom followed by ionization of the resulting ion.

IV. SUMMARY

As promised in the Introduction, the examination of single and double multiphoton ionization of a two-electron model atom has led to several useful insights. For high-frequency, short-pulse, laser-atom interactions, the electron ionization processes are well described by rather modest lattice ranges. This bodes well for the development of full 3D calculations of the helium atom. The lattice range may become more of a factor, however, for lower frequencies, longer pulses, and especially when describing harmonic generation and above-threshold ionization. Electron ionization processes were found to be sensitive to the frequency and the intensity of the radiation field. Resonant processes may retard the general increase in ionization yield at the stronger intensities. The intensity at which we found an unmistakable double-ionization signal coincided with a nontrivial contribution from the sequential process of escape from an already once ionized atom. Finding an unmistakable nonsequential double-ionization signal at lower intensities may prove difficult for lattice methods.

The time-dependent unrestricted Hartree-Fock approximation was found to be in qualitative agreement with the more exact direct solution method for the various electron ionization processes. However, at the highest intensity the TDUHF method found five times less single ionization with excitation than the TDSE method. Also, the angular distributions of the double-ionization probability densities for the two methods were quite distinct. Due to the complexity of the TDUHF formulation and its less than satisfying agree-

ment in the model atom comparisons, we are reluctant to recommend its application to a full 3D calculation of the helium atom.

In conclusion, we feel that a direct solution of the time-dependent Schrödinger equation for high-frequency, short-pulse, laser atom interactions may be effectively employed to examine single- and double-electron-ionization processes in real atomic systems. The extension of such an approach to lower frequencies, longer pulses, and lower intensities still needs further work at the model atom level.

ACKNOWLEDGMENTS

In this work M.S.P. and P.G. were supported in part by an NSF Grant (NSF-PHY-9122199) with Auburn University and F.R. was supported in part by an NSF Young Investigator Grant (NSF-PHY-9457903) with Auburn University. Computational work was carried out at the National Energy Research Supercomputer Center in Livermore, California, and the Alabama Supercomputer Center in Huntsville, Alabama.

[1] J. M. Bizau and F. J. Wuilleumier, J. Electron Spectrosc. Relat. Phenom. **71**, 205 (1995).
[2] S. L. Carter and H. P. Kelly, Phys. Rev. A **24**, 170 (1981).
[3] K. Hino, T. Ishihara, F. Shimizu, N. Toshima, and J. H. McGuire, Phys. Rev. A **48**, 1271 (1993).
[4] D. Proulx and R. Shakeshaft, Phys. Rev. A **48**, R875 (1993).
[5] K. W. Meyer and C. H. Greene, Phys. Rev. A **50**, R3573 (1994).
[6] C. Pan and H. P. Kelly, J. Phys. B **28**, 5001 (1995).
[7] J. M. Rost, Phys. Rev. A **53**, R640 (1996).
[8] B. Walker, B. Sheehy, L. F. DiMauro, P. Agostini, K. J. Schafer, and K. C. Kulander, Phys. Rev. Lett. **73**, 1227 (1994).
[9] D. N. Fittinghoff, P. R. Bolton, B. Chang, and K. C. Kulander, Phys. Rev. Lett. **69**, 2642 (1992).
[10] A. Becker and F. H. M. Faisal, J. Phys. B **29**, L197 (1996).
[11] P. Corkum, Phys. Rev. Lett. **71**, 1994 (1993).
[12] M. S. Pindzola, D. C. Griffin, and C. Bottcher, Phys. Rev. Lett. **66**, 2305 (1991).
[13] M. S. Pindzola, P. Gavras, and T. W. Gorczyca, Phys. Rev. A **51**, 3999 (1995).
[14] R. Grobe and J. H. Eberly, Phys. Rev. Lett. **68**, 2905 (1992).
[15] R. Grobe and J. H. Eberly, Phys. Rev. A **48**, 4664 (1993).
[16] S. L. Haan, R. L. Grobe, and J. H. Eberly, Phys. Rev. A **50**, 378 (1994).
[17] D. R. Schultz, C. Bottcher, D. H. Madison, J. L. Peacher, G. Buffington, M. S. Pindzola, T. W. Gorczyca, P. Gavras, and D. C. Griffin, Phys. Rev. A **50**, 1348 (1994).
[18] S. Chelkowski and A. D. Bandrauk, J. Phys. B **28**, L1 (1995).
[19] K. C. Kulander, F. H. Mies, and K. J. Schafer, Phys. Rev. A **53**, 2562 (1996).
[20] J. Parker, K. T. Taylor, C. W. Clark, and S. Blodgett-Ford, J. Phys. B **29**, L33 (1996).
[21] F. Robicheaux, C. T. Chen, P. Gavras, and M. S. Pindzola, J. Phys. B **28**, 3047 (1995).
[22] D. W. Peaceman and H. H. Rachford, J. Soc. Indust. Appl. Math. **3**, 28 (1955).
[23] C. Bottcher, G. J. Bottrell, and M. R. Strayer, Comput. Phys. Commun. **63**, 63 (1991).